

## Fatigue life prediction of gas metal arc welded cruciform joints of AA7075 aluminium alloy failing from root region

B. RAVINDRA<sup>1</sup>, T. SENTHIL KUMAR<sup>2</sup>, V. BALASUBRAMANIAN<sup>3</sup>

1. Department of Mechanical Engineering, Dr. Ambedkar Institute of Technology,  
Near Jnana Bharathi Campus, Bangalore 560056, India;

2. Department of Mechanical Engineering, Anna University-Tiruchirappalli, Tiruchirappalli 620024, India;

3. Centre for Materials Joining & Research (CEMAJOR), Department of Manufacturing Engineering,  
Annamalai University, Annamalainagar 608 002, India

Received 22 July 2010; accepted 10 January 2011

**Abstract:** Empirical relationship was developed to predict the fatigue life of gas metal arc welded (GMAW) cruciform joints failing from root region. High strength, age hardenable aluminium alloy of AA7075-T6 grade was used as the base material. The design of experiments concept was used to optimize the required number of fatigue testing experiments. Fatigue experiment was conducted in a servo hydraulic controlled fatigue testing machine under constant amplitude loading. The empirical relationship was developed. By using the developed empirical relationship, the fatigue life of GMAW cruciform joints failing from root region was predicted at 95% confidence level. The effect of cruciform joint dimensions on fatigue life was discussed in detail.

**Key words:** aluminium alloy; gas metal arc welding; cruciform joint; fatigue life

### 1 Introduction

High strength Al-Zn-Mg-Cu aluminium alloys have gathered wide acceptance in the fabrication of light weight structures requiring a high strength-to-mass ratio, such as transportable bridge girders, military vehicles, road tankers and railway transport systems. The preferred welding processes of high strength aluminium alloy are gas metal arc welding (GMAW) and gas tungsten arc welding (GTAW) due to their comparatively easier applicability and better economy. Fillet welds are the most common ones in the metal work of construction and machines. In machine building as a whole, their share is up to 80%. In ship hull structures, joints with fillet welds also prevail and their share is up to 85%. The wide application of fillet welds in various structures including off-shore and nuclear installations gives large scope for the researchers to analyze their behavior under different types of loading [1].

Linking the effects of welding defects and failure analysis of weldments pointed out that the fatigue alone is considered to account for most of the disruptive

failures and often precedes the onset of brittle [2]. The fatigue resistance of weld metal and heat affected zone of various steels is better or equal to the base metal. However, problems arise when there is an abrupt change in section by excess weld reinforcement, undercut, inclusion of slag or lack of penetration or fusion [3]. The fatigue crack growth behavior of welded joints depends on the material, loading and in particular, the geometric configurations of the weld and plate [4].

Two types of cracking normally will cause failure of a fillet welded joint. They are root cracking and toe cracking. In cruciform joints, a commonly encountered defect is lack of penetration (LOP), which occurs in the joint due to lack of access to the root region during fabrication. The structures in which such joints present are often subjected to a fatigue type of loading. This may result in the initiation of a fatigue crack at the LOP defect, and the propagation of such cracks in the weld metal will result in the failure of the joint. The lack of penetration defect will affect the fatigue behaviour of a fillet weld when its size exceeds a critical value of half of the plate thickness to be welded. The root failure can not be prevented unless the weld dimensions are made

appropriate to the plate thickness [5].

Fatigue life prediction of welded joints is complex costly and time consuming. This is due to the multiplicity of stress concentration locations and heterogeneity of the weld metal properties. The traditional approach is to apply the  $S-N$  curve as described in BS 5400 or in IIW documents [6]. However, the fatigue life estimation of a welded joint with defects can be made by performing a crack growth and subsequently evaluating the fatigue life in terms of crack growth parameters such as  $da/dN$  versus  $\Delta K$ . Such data merely indicate the fatigue crack growth behavior of the component and do not predict the actual fatigue life [7]. Inverse first-order reliability method was used to evaluate the fatigue life at an arbitrary reliability level [8]. No literature has been found to predict the fatigue life of GMAW cruciform joints of AA7075 aluminium alloy failing from root region. Hence, in this investigation an attempt has been made to develop empirical relationship to predict the fatigue life of GMAW cruciform joints failing from root region using statistical tools such as design of experiments, analysis of variance and regression analysis.

## 2 Scheme of investigation

In order to achieve the desired aim, the investigations were planned in the following sequences:

- 1) Identifying the predominant factors (joint dimensions) that have influence on the fatigue life of the cruciform joints;
- 2) Finding the upper and lower limits of chosen factors;
- 3) Developing the experimental design matrix.
- 4) Fabricating the joints and preparing the specimens;
- 5) Conducting the experiments as per the design matrix;
- 6) Developing the empirical relationship;
- 7) Checking the adequacy of the developed empirical relationship.

### 2.1 Identifying predominant factors

From Refs. [9–11], the predominant factors, which have influence on the fatigue life of cruciform joints, were identified. They are: 1) the ratio of the initial LOP size ( $2a$ ) to fillet width ( $2W$ ), 2) the ratio of leg length ( $L$ ) to plate thickness ( $T_p$ ), 3) fillet angle ( $\theta$ ) or weld profile and 4) stress range ( $\Delta\sigma$ ).

### 2.2 Findings limits of predominant factors

From the analysis of a large number of fatigue crack growth experimental results carried out in our laboratory, the following conditions existed:

- 1) If the  $a/W$  ratio is less than 0.25, then the toe failure is predominant;
- 2) If the  $a/W$  ratio is between 0.25 and 0.45, then the root (LOP) failure is more common;
- 3) If the  $a/W$  ratio is greater than 0.45, then the failure occurs quickly ( $<10^4$  cycles), i.e. the failure is considered to be low cycle fatigue (LCF) failure;
- 4) If the  $L/T_p$  ratio is less than 0.6, then failure occurs much faster, like in the previous conditions;
- 5) If the  $L/T_p$  ratio is between 0.6 and 1.0, then the failure occurs from root (LOP) region;
- 6) If the  $L/T_p$  ratio is greater than 1.0, then the failure occurs from the toe region only;
- 7) If the weld profile is either concave ( $\theta < 25^\circ$ ) or straight ( $\theta > 45^\circ$ ), then failure occurs from the root (LOP) region;
- 8) If the weld profile is convex ( $\theta > 45^\circ$ ), then the toe cracking is predominant;
- 9) If the stress range is less than 50 MPa, then most of the specimens endure up to  $10^7$  cycles;
- 10) If the stress range is greater than 150 MPa, then majority of the specimens fail within  $10^4$  cycles (LCF region).

By considering all the aforesaid conditions, the feasible limits of the factors were chosen in such a way that the failure occurs in LOP region and in high cycle fatigue ( $> 10^4$  cycles) region and they are presented in Table 1. For the convenience of recording and processing the experimental data, the upper and lower of the factors are coded as +2 and -2, respectively, and the coded values of any intermediated levels can be calculated by using the expression [12].

$$X_1 = \frac{2X - (X_{\max} + X_{\min})}{X_{\max} - X_{\min}} \quad (1)$$

where  $X_1$  is the required value of a factor of any value  $X$  from  $X_{\min}$  to  $X_{\max}$ ;  $X_{\min}$  is the lower level of the factor and  $X_{\max}$  is the upper level of the factor.

**Table 1** Important factors and their levels

No.	Parameter	Notation	Level				
			-2	-1	0	+1	+2
1	$a/W$	$A$	0.25	0.3	0.35	0.40	0.45
2	$L/T_p$	$B$	0.60	0.70	0.80	0.90	1.00
3	$\theta/^\circ$	$P$	25	30	35	40	45
4	$\Delta\sigma/\text{MPa}$	$S$	50	75	100	125	150

### 2.3 Developing experimental design matrix

Owing to slightly wider ranges of the factors, it was decided to use a five-level, central composite, rotatable design matrix to optimize the experimental conditions. Table 2 shows the three sets of the coded conditions used to form the design matrix. The first 16 experimental

conditions (rows) were formed for the main effects by using the formula  $2^{n_c-1}$  for the low (-1) and high (+1) values, where ' $n_c$ ' refers to the column number. For example, in Table 2, the first four rows are coded as -1 and the next four rows are coded as +1, alternatively, in the third column ( $n_c=3$  and  $2^{3-1}=4$ ). All chosen variables at the intermediate level (0) constitute the centre points and the combination of each of the variable at either its lowest (-2) or highest (+2) with the other three variables of the intermediate levels constitute the star points. The method of designing such as matrix was dealt with elsewhere [12–13].

### 3 Experimental

#### 3.1 Fabricating joints and preparing specimens

A high strength, age hardenable aluminium alloy of

AA7075-T6 grade in the form of rolled plates of 8 mm thickness was used as the base material throughout the investigation. The rolled plates were cut into the required sizes and profiles by power hacksaw cutting and grinding. The initial joint configuration was obtained by securing the long plate (300 mm×100 mm) and the stem plate (300 mm×75 mm) in a cruciform position using tack welding. Subsequently, fillets were made between the long plate and stem plates by lying weld metal using GMAW process with matching consumables (Al-5%Mg alloy). All necessary care was taken to avoid joint distortion and the joints were made without applying any clamping devices. The chemical composition and mechanical properties of base metal and weld metals are presented in Tables 3 and 4.

Partial penetration joints were made in an identical manner, leaving an infused gap between each pair of

**Table 2** Design matrix and experimental results

Expt. No	Coded value				Original value				Fatigue life, $N_f/10^5$
	<i>A</i>	<i>B</i>	<i>P</i>	<i>S</i>	<i>A</i>	<i>B</i>	<i>P</i>	<i>S</i>	
1	-1	-1	-1	-1	0.3	0.70	30	75	4.36
2	+1	-1	-1	-1	0.4	0.70	30	75	2.82
3	-1	+1	-1	-1	0.3	0.90	30	75	7.65
4	+1	+1	-1	-1	0.4	0.90	30	75	5.34
5	-1	-1	+1	-1	0.3	0.70	40	75	4.56
6	+1	-1	+1	-1	0.4	0.70	40	75	3.33
7	-1	+1	+1	-1	0.3	0.90	40	75	5.82
8	+1	+1	+1	-1	0.4	0.90	40	75	3.96
9	-1	-1	-1	+1	0.3	0.70	30	125	0.36
10	+1	-1	-1	+1	0.4	0.70	30	125	0.81
11	-1	+1	-1	+1	0.3	0.90	30	125	3.00
12	+1	+1	-1	+1	0.4	0.90	30	125	2.01
13	-1	-1	+1	+1	0.3	0.70	40	125	0.51
14	+1	-1	+1	+1	0.4	0.70	40	125	0.57
15	-1	+1	+1	+1	0.3	0.90	40	125	0.99
16	+1	+1	+1	+1	0.4	0.90	40	125	0.30
17	-2	0	0	0	0.25	0.80	35	100	3.91
18	+2	0	0	0	0.45	0.80	35	100	1.50
19	0	-2	0	0	0.35	0.60	35	100	1.20
20	0	+2	0	0	0.35	1.00	35	100	4.79
21	0	0	-2	0	0.35	0.80	25	100	3.90
22	0	0	+2	0	0.35	0.80	45	100	1.91
23	0	0	0	-2	0.35	0.80	35	50	7.02
24	0	0	0	+2	0.35	0.80	35	150	0.30
25	0	0	0	0	0.35	0.80	35	100	4.00
26	0	0	0	0	0.35	0.80	35	100	3.42
27	0	0	0	0	0.35	0.80	35	100	3.37
28	0	0	0	0	0.35	0.80	35	100	4.01
29	0	0	0	0	0.35	0.80	35	100	3.96
30	0	0	0	0	0.35	0.80	35	100	3.37

**Table 3** Chemical composition of base metal and filler metal (mass fraction, %)

Material	Composition/%								
	Zn	Mg	Mn	Fe	Si	Cu	Cr	Ti	Al
Base metal (AA7075)	5.6	4.5	0.03	0.29	0.08	1.6	–	0.02	Bal.
Filler metal (AA5356)	0.1	5.0	0.12	0.40	0.25	0.10	0.12	0.20	Bal.

**Table 4** Mechanical properties of base metal and filler metal

Material	Yield strength/MPa	Tensile strength/MPa	Elongation/%	Vickers hardness (VHN)
Base metal (AA 7075)	410	480	4.72	140
Filler metal (AA 5356)	305	376	4.50	121

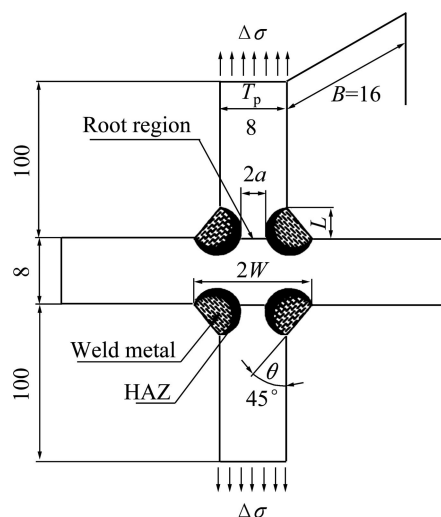
**Table 5** Welding conditions and process parameters

Parameter	Value
Welding machine	THYRO MIG–400, Lincoln, USA
Filler metal	AA 5356 (Al-5%Mg)
Filler diameter/mm	1.2
Arc voltage/V	22
Welding current/A	140
Welding speed/(mm·s <sup>-1</sup> )	4.0
Polarity	Alternating current (AC)
Heat input/(kJ·mm <sup>-1</sup> )	1.8
Preheat temperature/°C	100
Interpass temperature/°C	100
Shielding gas	Argon (99.99% purity)
Gas flow rate/(L·min <sup>-1</sup> )	14

fillets. This gap was termed as lack of penetration defect, and the length of the LOP was controlled by providing appropriate root faces, obtained by prior machining (by beveling). The various root faces enabled the joints to have different LOP lengths ( $2a$ ) and hence different crack lengths after welding. The LOP defect is a planar defect and more common in fillet welds owing to lack of access to the root region during welding [10]. The main objective of choosing this geometry was to study the root cracking failure of the cruciform joints. The fillet leg length ( $L$ ) was varied by controlling the number of weld passes. Weld profile (or fillet angle) was varied by controlling the electrode to work piece angle and arc length. Then the cruciform specimens were sliced from the joints to the dimensions (as shown in Fig. 1). The welding conditions and process parameters used in the fabrication of cruciform joints are given in Table 5.

### 3.2 Conducting experiments as per design matrix

The fatigue experiments were conducted as per the conditions dictated by the design matrix (Table 2) by

**Fig. 1** Dimensions of welded cruciform joint with LOP

using a servo hydraulic controlled fatigue testing machine of 100 kN capacity (8801–INSTRON, UK) with a frequency of 10 Hz under constant amplitude loading ( $R=0$ ). Care was taken to see that the load was axial and that no bending component was present in the joint. After the specimen was gripped between upper and lower gripping arrangement, pulsating load was applied to the specimen. The number of cycles to complete failure was recorded and presented in Table 2. Under each experimental condition, three specimens were tested and the average values were presented. Even though the experiments were conducted in a random order, Table 2 shows the standard order to avoid systematic error influencing the results.

## 4 Developing empirical relationship

Response surface methodology (RSM) is a collection of mathematical and statistical techniques that is useful for the modeling and analysis of problems in which a response of interest is influenced by several variables and the objective is to optimize this response. It has been provided by several researchers [14–17]. The response function, the fatigue life of welded cruciform joints containing LOP defects by  $N_f$ , can be expressed as [18]

$$N_f = f(a/W, L/T_p, \theta, \Delta\sigma) = f(A, B, P, S) \quad (2)$$

The second order polynomial (regression) equation used to represent the response surface ‘ $Y$ ’ is given by

$$Y = b_0 + \sum b_i x_i + \sum b_{ii} x_i^2 + \sum b_{ij} x_i x_j + e_r \quad (3)$$

and for four factors, the selected polynomial could be expressed as

$$N_f = b_0 + b_1(A) + b_2(B) + b_3(P) + b_4(S) + b_{11}(A^2) + b_{22}(B^2) + b_{33}(P^2) + b_{44}(S^2) + b_{12}(AB) + b_{13}(AP) + b_{14}(AS) + b_{23}(BP) + b_{24}(BS) + b_{34}(PS) \quad (4)$$

where  $b_0$  is the average of responses, and  $b_1, b_2, \dots, b_{34}$  are the coefficients that depend on respective main and interaction effects of the parameters.

In order to estimate the regression coefficients, a number of experimental design techniques are available. In this work, central composite design was used which fits the second order response surface very accurately. All the coefficients were obtained by applying central composite design using the Design Expert statistical software package. After determining the significant coefficient, the final relationship was developed using

only these coefficients. The empirical relationship to predict the fatigue life of gas tungsten arc welded cruciform joints of AA7075 aluminium alloy is given below:

$$N_f = (3.688 - 0.539A + 0.789B - 0.429P - 1.780S - 0.224AB + 0.361AS - 0.472BP - 0.228BS - 0.274A^2 - 0.201B^2 - 0.224P^2) \times 10^5$$

The adequacy of the developed relationship was tested using the analysis of variance technique (ANOVA). As per this technique, if the calculated value of the  $F_{\text{ratio}}$  of the developed relationship is less than the standard  $F_{\text{ratio}}$  (from  $F$ -table) value at a desired level of confidence (95%), then the relationship is said to be adequate within the confidence limit. ANOVA test results are presented in Table 6. From Table 6, it is understood that the developed relationship is found to be adequate at 95% confidence level.

The model  $F$ -value of 99.814 65 implies that the relationship is significant. There is only a 0.01% chance since  $p$ -value  $\text{prob} > F$  is less than 0.000 1, for a failure to occur due to noise. Values of “ $\text{Prob} > F$ ” less than

**Table 6** ANOVA test results

Source	Sum of squares	df	Mean square	$F$ value	$p$ -value $\text{prob} > F$	Significance
Model	113.412 6	14	8.100 902	99.814 65	< 0.000 1	Significant
$A$ - $A$ *	6.966 038	1	6.966 038	85.831 51	< 0.000 1	
$B$ - $B$ *	14.931 04	1	14.931 04	183.971 7	< 0.000 1	
$P$ - $P$ *	4.411 838	1	4.411 838	54.360 12	< 0.000 1	
$S$ - $S$ *	76.077 2	1	76.077 2	937.379 6	< 0.000 1	
$AB$ *	0.805 506	1	0.805 506	9.9249 85	0.006 6	
$AP$	0.028 056	1	0.028 056	0.345 693	0.565 3	
$AS$ *	2.080 806	1	2.080 806	25.638 5	0.000 1	
$BP$ *	3.562 656	1	3.562 656	43.897	< 0.000 1	
$BS$ *	0.832 656	1	0.832 656	10.259 51	0.005 9	
$PS$	0.107 256	1	0.107 256	1.321 55	0.268 3	
$A^2$ *	2.053 907	1	2.053 907	25.307 07	0.000 1	
$B^2$ *	1.109 75	1	1.109 75	13.673 7	0.002 1	
$P^2$ *	1.371 907	1	1.371 907	16.903 85	0.000 9	
$S^2$	0.033 4	1	0.033 4	0.411 539	0.530 9	
Residual	1.217 392	15	0.081 159			
Lack of fit	0.668 308	10	0.066 831	0.608 567	0.764 5	Not significant
Pure error	0.549 083	5	0.109 817			
Cor total	114.63	29				
Std. dev.	0.284 885		$R^2$	0.989 38		
Mean	3.101 667		Adj $R^2$	0.979 468		
CV	9.184 9%		Pred $R^2$	0.959 521		
Press	4.640 136		Adeq $R^2$	38.466 01		

df: Degrees of freedom; CV: Coefficient of variation;  $F$ : Fisher ratio;  $\text{prob} > F$ : probability; \* significant factor

0.050 0 indicate relationship terms are significant. In this case,  $A, B, P, S, AB, AS, BP, BS, A^2, B^2, P^2$  are significant model terms. Values greater than 0.1 indicate the relationship terms are not significant. The “Lack of Fit  $F$ -value” of 0.608 567 implies that the lack of fit is not significant relative to the pure error. Coefficient of determination “ $R^2$ ” is used to find how close the predicted and experimental values. The value of “ $R^2$ ” for the above-developed relationship is also presented in Table 6, which indicates high correlation exists between the experimental and predicted values. The “Pred  $R^2$ ” of 0.959 521 is in reasonable agreement with the “Adj  $R^2$ ” of 0.979 468. “Adeq Precision” measures the signal to noise ratio. The normal probability plot of the residuals for fatigue life is shown in Fig. 2, which reveals that the residuals are falling on the straight line, which means the errors are distributed normally (KUMAR et al, 2007). All the above consideration indicates an excellent adequacy of the developed empirical relationship. Each observed value is compared with the predicted value calculated from the relationship shown in Fig. 3.

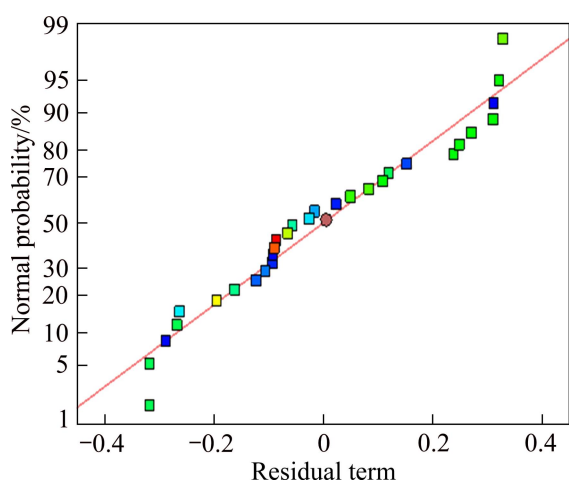


Fig. 2 Normal probability plot

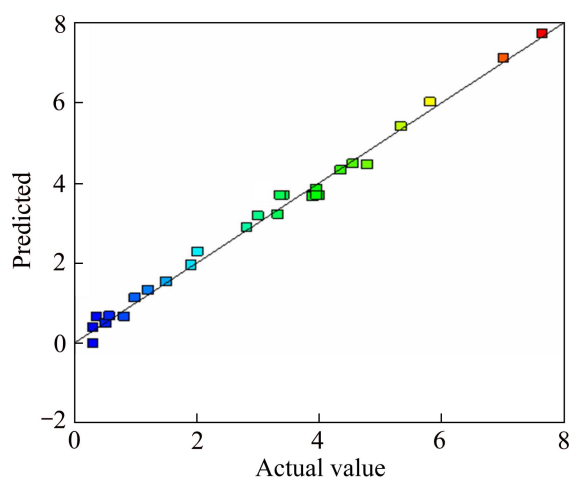


Fig. 3 Correlation graph

## 5 Discussion

Using the developed empirical relationship, the fatigue lives were predicted for different combinations of joint dimensions and they are presented in the graphical form (Fig. 4). The effects of joint dimensions on fatigue life are discussed in the following sections.

### 5.1 Effect of $L/T_p$ ratio on fatigue life

The  $L/T_p$  ratio, i.e. the ratio between leg length and plate thickness, decides the final weld size of the cruciform joints. The effect of  $L/T_p$  ratio on fatigue life for different values of LOP size and fillet angle is shown in Fig. 4. From Fig. 4, it is evident that the higher the  $L/T_p$  ratio is, the larger the fatigue lives will be and vice versa. The reason can be easily understood from the following stress intensity factor (SIF) range expression, for a load carrying cruciform joint at the apex of a root (LOP) defect [19].

$$\Delta K = \frac{\Delta\sigma[A_1 + A_2a^*][\pi a \sec(a^*/2)]^{1/2}}{[1 + 2(L/T_p)]} \quad (5)$$

where  $\Delta\sigma$  is the nominal stress;  $a$  is the half crack length;  $a^*(=a/W)$  is the normalized crack length;  $L/T_p$  is the weld size;  $A_1$  and  $A_2$  are constants which depend on the weld size. From the above expression, it is clear that the SIF range is inversely proportional to the  $L/T_p$  ratio, i.e. if the  $L/T_p$  ratio is more (for larger welds), the SIF range value will become low and hence the crack initiation, crack propagation and failure will be delayed. More importantly, the variations in the fatigue crack growth behaviour and fatigue life are mainly attributed to the difference in the number of weld passes involved during the fabrication of the joints. Further, the larger welds have more weld metals and hence the fatigue crack has to propagate longer distance before final failure to occur.

### 5.2 Effect of $a/W$ ratio on fatigue life

The  $a/W$  ratio, i.e. the ratio between the initial LOP size and the filler width, decides the defect size in cruciform joints. The effect of LOP size on fatigue life for different values of  $L/T_p$  is depicted in Fig. 4. From Fig. 4, it is clear that the lower the LOP size is, the higher the fatigue life will be and vice versa for any weld size and fillet angle. This is caused by the fact that the joints containing smaller defects will give longer life than its counterpart. It is also evident from the SIF range expression, given earlier, that the SIF range value is directly proportional to the  $a/W$  ( $a^*$ ) and hence the joint with smaller LOP defect will endure more number of cycles than its counterpart. If the LOP defect size is

small, then crack initiation will be delayed as a result of the lower values of SIF range, but the reverse will be the result if the LOP defect size is large. Moreover, the crack has to propagate comparatively smaller distance when  $a/W$  is larger due to the reduced effective fillet width.

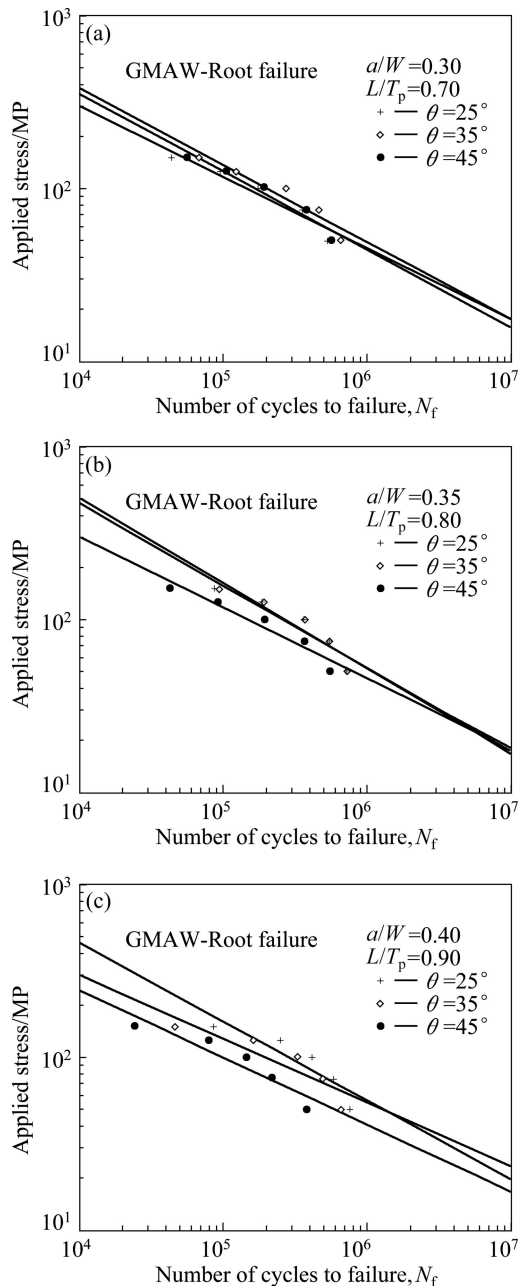


Fig. 4 Effect of cruciform joint dimensions on fatigue life

### 5.3 Effect of weld profile on fatigue life

The fillet angle will decide the weld profile in cruciform joints. Figure 4 reveals the effect of weld profile on fatigue life of cruciform joints, for various  $L/T_p$  and  $a/W$  values. From Fig. 4, it is inferred that the straight fillets ( $\theta=45^\circ$ ) are superior compared to concave fillets but the difference is very small. This can be easily understood from the following SIF range expression for the cracks emanating from the toe region [20]:

$$\Delta K = \frac{[M_s \cdot M_t \cdot M_k \cdot \Delta \sigma (\pi a)^{1/2}]}{\Phi_0} \quad (6)$$

where  $M_s$  is the correction factor for the effect of free surface;  $M_t$  is the correction factor for the effect of plate thickness;  $M_k$  is the correction factor for the effect of stress concentration owing to the weld toe angle;  $\Phi_0$  is the correction factor for the effect of crack front shape.

From the above expression, it is obvious that the fillet toe angle is directly proportional to the SIF range values at weld toe. In load carrying cruciform joint, if the fillet angle is more than  $45^\circ$ , then the SIF range is sufficient to initiate and propagate a fatigue crack and cause failure in the joint prematurely as a result of its high level of stress concentration effect near the toe region. If the fillet angle is less than  $45^\circ$ , then the SIF range is not sufficient to initiate a fatigue crack from toe region but the SIF range at the tip of LOP defect is increased as a result of the reduction in effective weld size. Further, in the concave fillets, less weld metal is available to resist the propagation of fatigue crack and hence the failure occurs somewhat earlier than in the straight fillet welds.

## 6 Conclusions

1) An empirical relationship was developed to predict the fatigue life of load carrying gas metal arc welded cruciform joints of AA7075 aluminium alloy failing from root region incorporating joint dimensions.

2) The developed empirical relationship can be effectively used to predict the fatigue life of load carrying gas metal arc welded cruciform joints failing from root region at 95% confidence level. However, the validity of the models is limited to the range of the factors considered in this investigation.

3) The effect of cruciform joint dimensions on fatigue life was analyzed in detail. Larger weld size and straight profile fillet welds show better fatigue performance compared to other combinations.

## Acknowledgements

The authors are grateful to the Centre for Materials Joining & Research (CEMAJOR), Department of Manufacturing Engineering, and Annamalai University for extending the facilities of Materials Joining Laboratory and Materials Testing Laboratory.

## References

- [1] YAKUBOVSKI V V, VALTERIS I I. Geometrical parameters of butt and fillet welds and their influence on the welded joint fatigue life [R]. IIW Doc, XIII: 1326–69. 1989.
- [2] TSAI C L. Fitness for service design of fillet welded joints [J]. J Struct Eng, 1986, 112(8): 1761–1780.

- [3] BLODGETT O W. Designing weldments for fatigue loading [J]. *Welding J*, 1992, 7: 39–42.
- [4] FRANK K H, FISHER J W. Fatigue strength of fillet welded cruciform joints [J]. *J Struct Div*, 1979, 105: 1727–1739.
- [5] VEEREMAN Y, BAILON J P, MASAUNOVE J. Fatigue life prediction of welded joints: A reassessment [J]. *Fatigue Fract Eng Mater Struct*, 1987, 10: 17–36.
- [6] OTEGUI J L, MOHAUPUT U H, BURNS D J. Effect of weld process on early growth of fatigue cracks in steel T-joints [J]. *Int J Fatigue*, 1991, 13(1): 45–58.
- [7] CHAPETTI M D, OTEGUI J L. Importance of toe irregularity for fatigue resistance of automatic welds [J]. *Int J Fatigue*, 1995, 17(8): 531–538.
- [8] XIANG Yi-bing, LIU Yong-ming. Application of inverse first-order reliability method for probabilistic fatigue life prediction [J]. *Prob Engg Mech*, 2011, 26: 148–156.
- [9] MADDOX S J. Recent advances in the fatigue assessment of weld imperfections [J]. *Welding J*, 1993, 72: 42–52.
- [10] HOBACHER A. Recommendations for fatigue design of welded joints and components [R]. IIW Doc, No. XIII-1939-96/XV-845-96. 1996.
- [11] USAMI S, KUSUMOTO S. Fatigue strength of cruciform, tee and lap joints [J]. *Trans Jpn Welding Soc*, 1978, 9: 1–10.
- [12] BOX G E P, HUNTER W H, HUNTER J S. *Statistics for experiments* [M]. New York: Wiley, 1978.
- [13] MILER I, FREUND J E. *Probability and statistics for engineers* [M]. New Delhi: Prentice-Hall of India, 1978.
- [14] GUNARAJ V, MURUGAN N. Application of response surface methodology for predicting weld bead quality in submerged arc welding of pipes [J]. *J Mater Process Technol*, 1999, 88: 266–275.
- [15] MANONMANI K, MURUGAN N, BUVANASEKARAN G. Effect of process parameters on the weld bead geometry of laser beam welded stainless steel sheets [J]. *J Joining Mater*, 2005, 17: 103–109.
- [16] BALASUBRAMANIAN M, JAYABALAN V, BALASUBRAMANIAN V. Developing mathematical models to predict tensile properties of pulsed current gas tungsten arc welded Ti-6Al-4V alloy [J]. *Mater Des*, 2008, 29: 92–97.
- [17] PALANI P K, MURUGAN N. Optimization of weld bead geometry for stainless steel claddings deposited by FCAW [J]. *J Mater Process Technol*, 2007, 190: 291–299.
- [18] MONTGOMERY D C. *Design and analysis of experiments* [M]. New York: Wiley, 1991.
- [19] GUHA B. Fatigue life estimate of C-Mn steel welded cruciform joints [J]. *Theoret App Fract Mech*, 1994, 21: 121–129.
- [20] FERREIRA J A M, BRANCO C M. Influence of welds and plate geometry on the fatigue strength of cruciform joints [J]. *Theoret Appl Fract Mech*, 1988, 9(1): 23–32.

## AA7075 铝合金熔化极气体保护焊 十字接头根部失效疲劳寿命的预测

B. RAVINDRA<sup>1</sup>, T. SENTHIL KUMAR<sup>2</sup>, V. BALASUBRAMANIAN<sup>3</sup>

1. Department of Mechanical Engineering, Dr. Ambedkar Institute of Technology,  
Near Jnana Bharathi Campus, Bangalore 560056, India;

2. Department of Mechanical Engineering, Anna University-Tiruchirappalli, Tiruchirappalli 620024, India;

3. Centre for Materials Joining & Research (CEMAJOR), Department of Manufacturing Engineering,  
Annamalai University, Annamalainagar 608 002, India

**摘要:** 通过建立一经验公式来预测熔化极气体保护焊十字接头根部失效的疲劳寿命。采用高强可时效硬化的 AA7075-T6 铝合金作为基材进行焊接实验。实验设计概念被用来优化进行疲劳实验所需要的次数。在一伺服液压控制疲劳试验机上进行疲劳实验，实验采用恒定荷载。采用所建立的经验公式，预测的熔化极气体保护焊十字接头根部失效疲劳寿命可达到 95% 的可信度水平。详细讨论了十字接头尺寸对疲劳寿命的影响。

**关键词:** 铝合金；熔化极气体保护焊；十字接头；疲劳寿命

(Edited by YUAN Sai-qian)